

# Microbial Abundance and Diversity in Subsurface Lower Oceanic Crust at Atlantis Bank, Southwest Indian Ridge

👵 Shu Ying Wee, ª 📵 Virginia P. Edgcomb, b David Beaudoin, b 📵 Shari Yvon-Lewis, a 📵 Jason B. Sylvana

<sup>a</sup>Department of Oceanography, Texas A&M University, College Station, Texas, USA

<sup>b</sup>Geology and Geophysics Department, Woods Hole Oceanographic Institution, Woods Hole, Massachusetts, USA

ABSTRACT International Ocean Discovery Program Expedition 360 drilled Hole U1473A at Atlantis Bank, an oceanic core complex on the Southwest Indian Ridge, with the aim of recovering representative samples of the lower oceanic crust. Recovered cores were primarily gabbro and olivine gabbro. These mineralogies may host serpentinization reactions that have the potential to support microbial life within the recovered rocks or at greater depths beneath Atlantis Bank. We quantified prokaryotic cells and analyzed microbial community composition for rock samples obtained from Hole U1473A and conducted nutrient addition experiments to assess if nutrient supply influences the composition of microbial communities. Microbial abundance was low (≤10<sup>4</sup> cells cm<sup>-3</sup>) but positively correlated with the presence of veins in rocks within some depth ranges. Due to the heterogeneous nature of the rocks downhole (alternating stretches of relatively unaltered gabbros and more significantly altered and fractured rocks), the strength of the positive correlations between rock characteristics and microbial abundances was weaker when all depths were considered. Microbial community diversity varied at each depth analyzed. Surprisingly, addition of simple organic acids, ammonium, phosphate, or ammonium plus phosphate in nutrient addition experiments did not affect microbial diversity or methane production in nutrient addition incubation cultures over 60 weeks. The work presented here from Site U1473A, which is representative of basement rock samples at ultraslow spreading ridges and the usually inaccessible lower oceanic crust, increases our understanding of microbial life present in this rarely studied environment and provides an analog for basement below ocean world systems such as Enceladus.

**IMPORTANCE** The lower oceanic crust below the seafloor is one of the most poorly explored habitats on Earth. The rocks from the Southwest Indian Ridge (SWIR) are similar to rock environments on other ocean-bearing planets and moons. Studying this environment helps us increase our understanding of life in other subsurface rocky environments in our solar system that we do not yet have the capability to access. During an expedition to the SWIR, we drilled 780 m into lower oceanic crust and collected over 50 rock samples to count the number of resident microbes and determine who they are. We also selected some of these rocks for an experiment where we provided them with different nutrients to explore energy and carbon sources preferred for growth. We found that the number of resident microbes and community structure varied with depth. Additionally, added nutrients did not shape the microbial diversity in a predictable manner.

**KEYWORDS** International Ocean Discovery Program, Southwest Indian Ridge, deep biosphere, gabbro, microbial ecology, ocean crust

he deep subseafloor biosphere in igneous basement remains one of the least explored ecosystems on Earth. Basaltic basement is representative of fast-spreading midocean ridges and the upper oceanic crust below the seafloor. To date, exploration of subseafloor basaltic basement such as the Juan de Fuca Ridge (1-7) and North Pond (8-12) has provided valuable insights into the diversity and activities of microorganisms in the upper oceanic Citation Wee SY, Edgcomb VP, Beaudoin D, Yvon-Lewis S, Sylvan JB. 2021. Microbial abundance and diversity in subsurface lower oceanic crust at Atlantis Bank Southwest Indian Ridge. Appl Environ Microbiol 87: e01519-21. https://doi.org/10.1128/AEM.01519-21.

Editor Jeremy D. Semrau, University of Michigan-Ann Arbor

Copyright © 2021 American Society for Microbiology. All Rights Reserved.

Address correspondence to Jason B. Sylvan, jasonsylvan@tamu.edu.

Received 28 July 2021 Accepted 26 August 2021

Accepted manuscript posted online

1 September 2021

Published 28 October 2021

crust. The lower oceanic crust lies below the upper oceanic crust, is comprised of the silicate rocks gabbro and peridotite, and is a potential host habitat for microbial life at depths where temperatures remain below 120°C (13, 14). Despite representing a volumetrically large potential ecosystem below the seafloor, the biosphere of lower ocean crust remains largely unsampled due to logistical challenges.

Integrated Ocean Drilling Program Expeditions 304 and 305 were the first to sample the deep biosphere in lower oceanic crust. Samples as deep as 1,300 m below seafloor (mbsf) collected from Atlantis Massif, in the north Atlantic Ocean, were found to host DNA biosignatures of a microbial ecosystem dominated by heterotrophs and putative hydrocarbon oxidizers (15). To obtain cell counts for samples from Expeditions 304 and 305, the interior portions of rock samples were added to ionic detergent treatments, followed by cell detachment with a vortex and supernatant filtration. Attempts to quantify microbial cells using these cell counting protocols were not successful, indicating low microbial density in this environment. More recently, shallow drilling (57 mbsf or less) at Atlantis Massif during International Ocean Discovery Program (IODP) Expedition 357 successfully revealed low biomass microbial populations in densities up to  $6.5 \times 10^{2}$  cells cm<sup>-3</sup> using density gradient centrifugation techniques (16). The diversity of microbiota within ultramafic rocks from Expedition 357 was also characterized using amplicon-based analysis of the 16S rRNA genes. This revealed uncultured prokaryotic communities belonging to Thermoplasmata, Acidobacteria, Acidimicrobiia, and Chloroflexi (17).

IODP Expedition 360 sampled lower oceanic crust exhumed at Atlantis Bank on the Southwest Indian Ridge (SWIR) (18, 19). The SWIR is one of the two slowest-spreading ridges in the world, with a full spreading rate of  $\sim$ 14 mm year<sup>-1</sup>; the Gakkel Ridge in the Arctic Ocean is the only other ultraslow-spreading ridge (19, 20). A key feature of ultraslow-spreading ridges is the presence of amagmatic rifts that expose mantle peridotite directly on the seafloor (20, 21). Amagmatic rifting also lifts the lower oceanic crust, which is typically too deep to sample in areas with crust formed at medium or fast-spreading rates, closer to the surface. This results in easier access to gabbro and peridotite at the seafloor as well as sampling of intact lower ocean crust below the seafloor via seafloor drilling.

Atlantis Bank lies 73 km south of the SWIR, exposing the largest known gabbro complex in the oceans (660 km<sup>2</sup>),  $\sim$ 700 m below sea level, thus providing convenient drilling access to an otherwise largely inaccessible environment. The microbiology of ultraslowspreading ridge crust had not been studied at either Gakkel Ridge or the SWIR prior to Expedition 360, although microbial communities have been studied on hydrothermal vents along these ridges and in nearby surface sediments (22-27). IODP Expedition 360 drilled Hole U1473A to a depth of 789.8 mbsf (19). Hole U1473A core samples are composed of a variety of gabbroic lithologies, from primitive olivine gabbros to evolved oxide-rich gabbros (19). This composition provides the necessary elements for serpentinization, which is the process of aqueous alteration of olivine and pyroxene. In the process of serpentinization, hydrogen, methane, and short-chain hydrocarbons are produced that can be metabolized by microorganisms (28-30). While active serpentinization was not detected during drilling of Hole U1473A or during previous visits to Atlantis Bank (19), some samples collected were partially serpentinized. The partial serpentinization observed may have occurred in the past at depths we sampled and/or may be currently occurring at deeper horizons than drilled at Hole U1473A.

Initial investigation of microbial diversity in 11 of the cored samples from Hole U1473A revealed low cell density, from below detection to  $\sim 10^4$  cells cm<sup>-3</sup>, and enzyme activity and mRNA evidence that some fraction of cells detected was viable/active (31). mRNA analysis suggested the presence of microbial communities with adaptations for recycling the low total organic carbon occurring in this environment (0.004 to 0.018 wt%) (31). Additionally, fungal communities were detected in samples from Hole U1473A as deep as 780 mbsf, and culture-based methods revealed that isolated fungi were able to use diverse carbon sources, including microbial lipids (32). Here, we present results of analysis of prokaryotic communities from samples spanning the entire cored depth of Hole

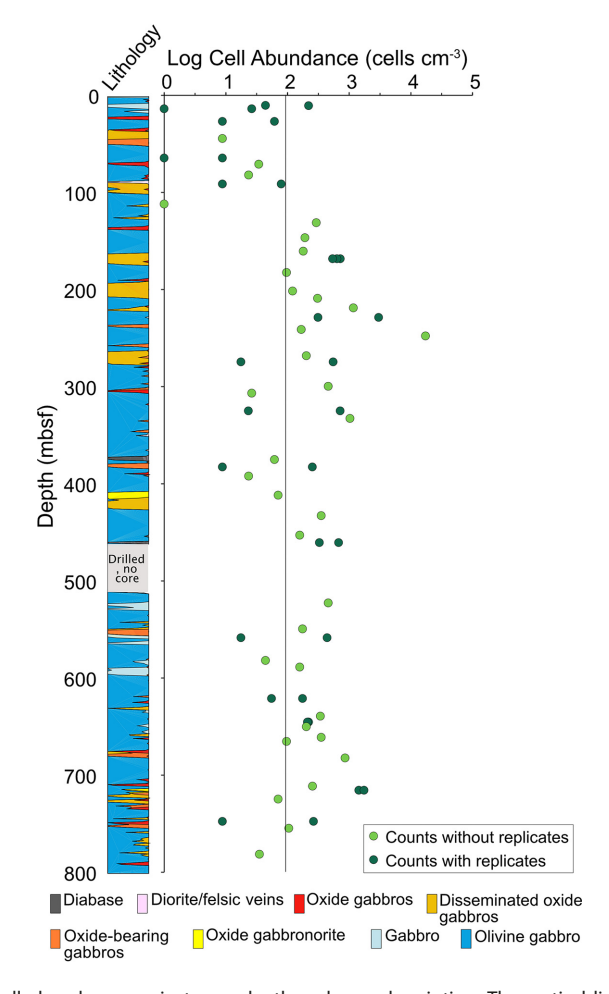


FIG 1 Plot of cell abundance against core depth and core description. The vertical line refers to limit of quantification,  $8.50 \times 10^{1}$  cells cm<sup>-3</sup>.

U1473A. We determined microbial cell counts for 51 samples and 16S rRNA gene diversity for 43 samples spanning from 10.73 to 781.45 mbsf. Additionally, we conducted nutrient addition incubation experiments using core material from 12 samples spanning the full depth range of Hole U1473A. From these nutrient addition incubations, microbial 16S rRNA gene diversity was analyzed and production of methane quantified. Profiling the microbial community present at Site U1437A up to 781.45 mbsf, which is representative of basement rock samples from potentially serpentinizing environments at slow- and ultraslow-spreading ridges, significantly expands our understanding of microbial life present in the lower oceanic crust, one of the most poorly explored habitats on Earth.

# **RESULTS**

Downhole cell abundance. Cell abundance was heterogeneously distributed and ranged from below detection in some samples to 10<sup>4</sup> cells cm<sup>-3</sup>, with an average of  $6.18 \times 10^2$  cells cm<sup>-3</sup> for all the samples from Hole U1473A (Fig. 1). Cell counts for roughly 30% of the samples analyzed were below the limit of quantification (8.50  $\times$  10<sup>1</sup> cells cm<sup>-3</sup>). For all samples from Hole U1473A, as well as for subsets of samples within depth ranges of every 100 m, correlation coefficients were calculated to obtain a statistical analysis of the relationship between cell abundance, carbonate vein frequency, and felsic vein frequency (Table S1a in the supplemental material). In addition, cell abundances were also compared to vein frequencies within depth ranges where three or more data points within that range were above the mean values for the whole data set for cell counts, carbonate vein frequency (>5 veins), felsic vein frequency (>8 veins), or total vein frequency (>12 veins) (Table S1b).

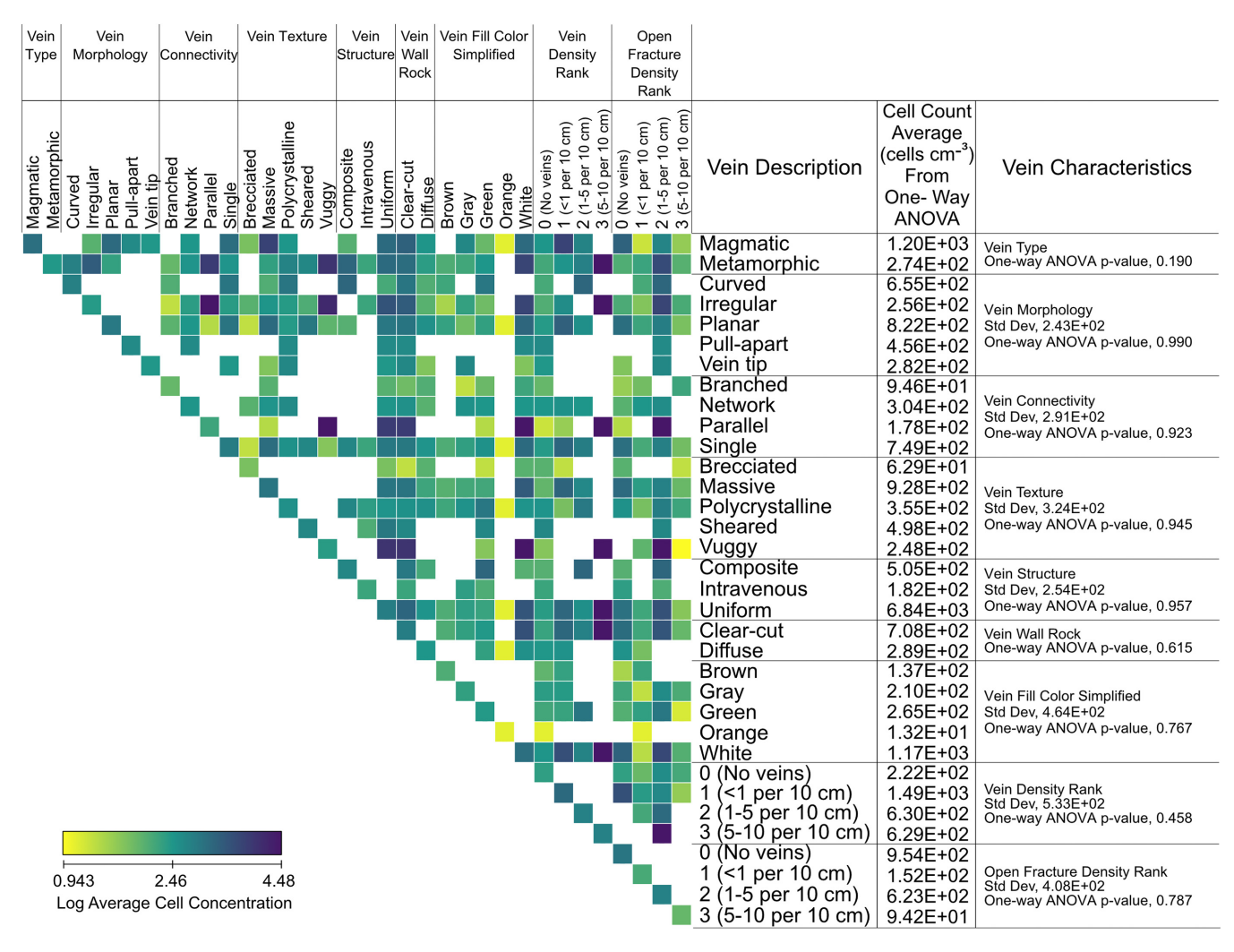


FIG 2 Log average cell concentration for each vein characteristic. One-way ANOVA within each major category is listed on the right.

Carbonate vein frequency showed a strong positive correlation with cell counts for depth ranges of 268.16 to 332.78 mbsf (correlation coefficient, 0.80;  $R^2$  value, 0.65). Felsic vein frequency also showed a strong positive correlation with cell counts from 411.74 to 460.64 mbsf (correlation coefficient, 0.93;  $R^2$  value, 0.87) and from 711.34 to 781.45 mbsf (correlation coefficient, 0.94;  $R^2$  value, 0.89). The effect of several other vein characteristics on cell counts was analyzed using a one-way analysis of variance (ANOVA) (Fig. 2; Table S2). These include vein type, morphology, connectivity, texture, structure, wall rock, fill color, density rank, and openfracture density rank. All categories returned P values of above 0.05. The effect of each vein description (e.g., two different descriptions of vein type are magmatic and metamorphic) within these categories on cell abundance was also not considered statistically significant.

Microbial community analysis of cores from Hole U1473A. After quality control steps to remove sequencing errors and amplicon sequence variants (ASVs) that were likely derived from contamination (see details in Materials and Methods), the final data set included 2,032 ASVs collectively comprised of 152,190 reads (Table S3). A total of 75.2% of the sequences were *Bacteria*, and 24.8% of the sequences were *Archaea*. Bacterial sequences were dominated by *Proteobacteria*, which constituted 43.8% of the sequences, followed by *Marinimicrobia* (18.1%). Archaeal sequences were comprised of three phyla, *Thaumarchaeota* (84.0% of archaeal sequences), *Euryarchaeota* (11.8%), and *Nanoarchaeota* (4.2%). On the order level, the taxa present in highest relative abundance for all prokaryotic sequences are *Nitrosopumilales* (20.2%), *Alphaproteobacteria* SAR11 clade (15.7%), *Marinimicrobia* SAR406 (13.7%), and *Deltaproteobacteria* SAR324 clade marine group B (6.1%) (Fig. 3). Several

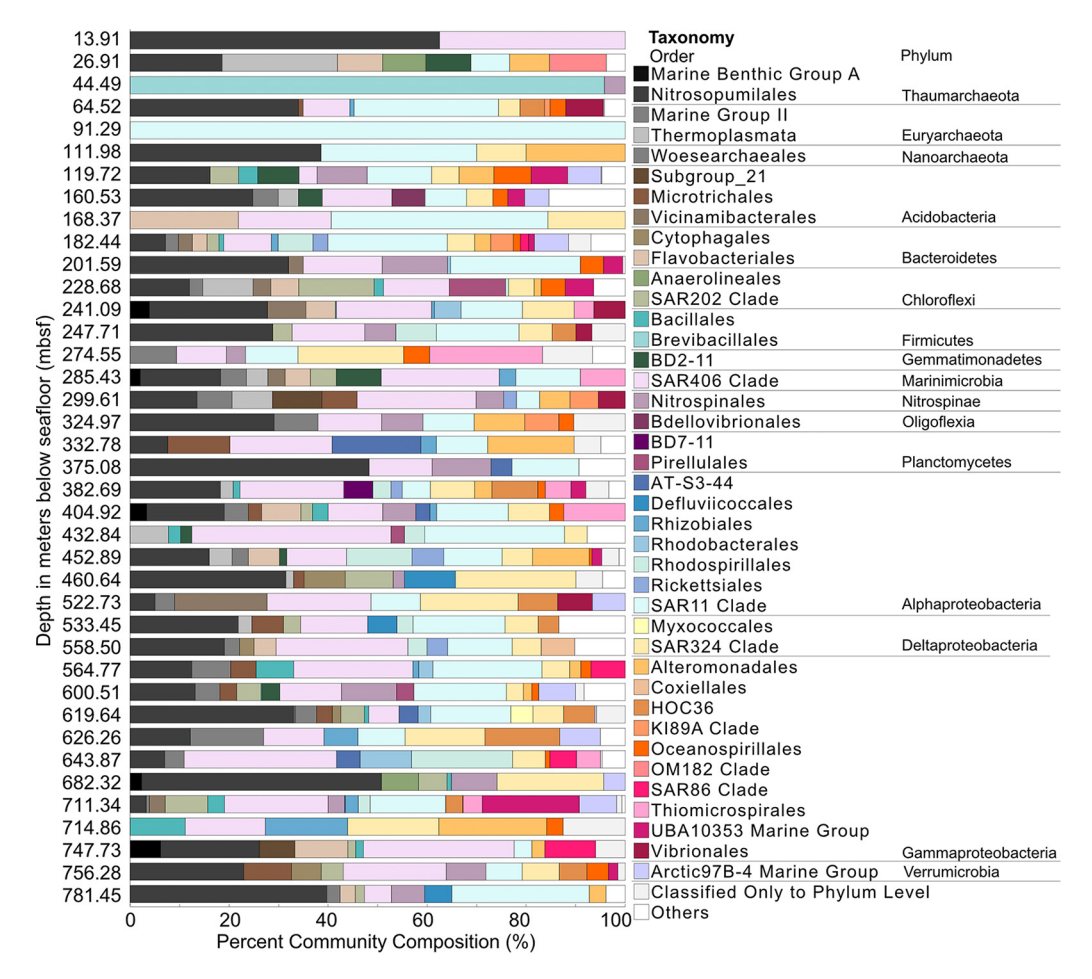
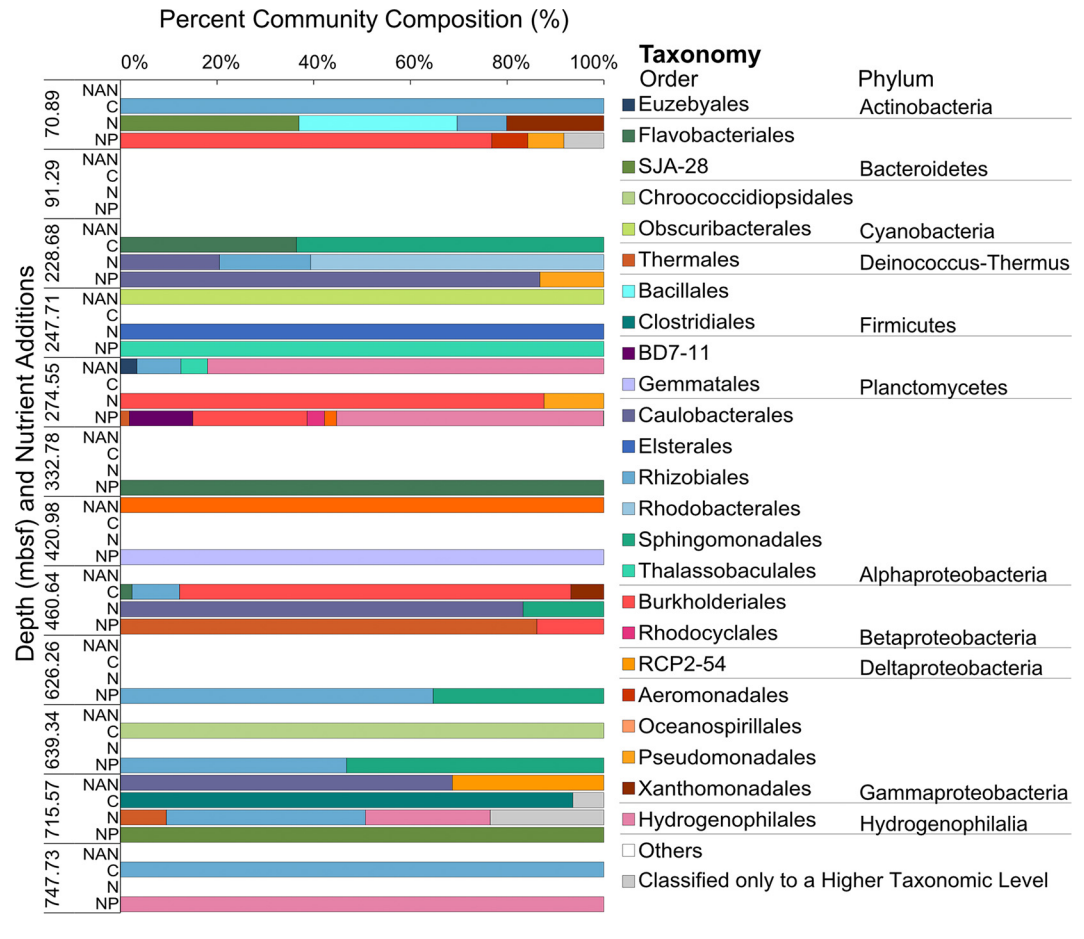


FIG 3 DNA-based microbial community composition for the core samples at the order and phylum taxonomic levels. The classes of Proteobacteria are listed as well. Community composition of samples from depths 10.73, 209.04, 306.65, and 420.98 mbsf was not listed, as there were no remaining ASVs after quality control.

Nitrosopumilales ASVs detected in these samples were found to be 99% similar to an uncultured archaeon clone sequenced from the hydrothermal plume and surrounding water mass above an active hydrothermal field on the Southwest Indian Ridge (33). The SAR11 ASVs from Atlantis Bank were 99% similar to uncultured bacterial clones from hydrothermal vents in the Southern Ocean as well as the water column of the Southwest Indian Ocean (34, 35). The SAR406 ASVs from the Atlantis Bank samples were 98.8% similar to uncultured bacterium clones from the water column of the Northeast Pacific Ocean (36).

ASV counts and diversity (inverse Simpson) within the U1473A core samples were calculated with respect to depth (Fig. S1). The highest ASV count and diversity were observed at 182.44 mbsf. No ASVs remained after quality control steps for depths 10.73, 209.04, 306.65, and 420.98 mbsf (Table S3; Fig. S1). The lowest calculated diversity was observed at 375.08 mbsf. Correlation coefficients were calculated for all depths and for depth ranges of every 100 m between diversity, carbonate vein frequency, felsic vein frequency, and total vein frequency (carbonate and felsic vein frequency combined) (Table S4). Within the 0- to 100-mbsf range, there were insufficient diversity data points for correlation calculation, as data were only available from 26.91 and 64.52 mbsf. For samples between 201.59 and 299.61, 404.92 and 460.64, and 711.34 and 781.45 mbsf, no positive correlation was observed between diversity and vein frequencies. For samples from 119.72 to 182.44 and 600.51 to 682.32 mbsf, there is a very strong positive correlation between diversity and felsic vein frequencies (correlation coefficients, 0.96 and 0.81; R<sup>2</sup> values, 0.81 and 0.65, respectively). Samples from 119.72 to 182.44 mbsf also showed a very strong positive correlation between diversity and carbonate vein frequency (correlation coefficient, 0.90; R<sup>2</sup> value,



**FIG 4** Microbial community composition for nutrient addition incubation experiments presented on the order and phylum taxonomic levels where all orders present over 1% relative abundance are displayed. NAN, no added nutrients; C, carbon (lactate, acetate, and formate) addition; N, ammonium addition; NP, ammonium and phosphate addition. The classes of *Proteobacteria* are listed as well.

0.81), and there was a moderate positive correlation with carbonate vein frequency for samples from 324.97 to 382.69 mbsf (correlation coefficient, 0.63;  $R^2$  value, 0.40). The correlation coefficient for diversity and total vein frequencies for samples from all depths show a negligible positive correlation (correlation coefficient, 0.12;  $R^2$  value, 0.015).

Analysis of community dissimilarity reveals no major grouping, and prokaryotic communities detected at each depth appear to be distinct from each other and scattered across the nonmetric multidimensional scaling (NMDS) plot (Fig. S3). Overall, there is no significant grouping by depth. One-way ANOVA returned P values of >0.05 for all the vein description categories, indicating no statistical significance for their effect on prokaryotic composition.

Microbial community analysis of nutrient addition incubation experiments. We conducted nutrient addition incubation experiments to test the hypothesis that added nutrients would stimulate microbial diversity and/or methane production in subseafloor ocean crust. Using samples from 12 depths, crushed rock chips were added to artificial seawater with no added nutrients (NAN), added ammonium (+N), added ammonium and phosphate (+NP), or added lactate, acetate, and formate (+C). After quality control steps (details in Materials and Methods), the data set for the final nutrient addition incubation community analysis included 57 ASVs comprised of 67,827 reads (Tables S5 and S6). Overall, nutrient addition incubations were dominated by *Proteobacteria*, which constituted 74.8% of the sequences, followed by *Cyanobacteria* (7.8%), *Bacteroidetes* (6.5%), *Firmicutes* (5.2%), and others (5.7%), which includes *Actinobacteria*, *Armatimonadetes*, *Deinococcus-Thermus*, and *Planctomycetes* (Fig. 4). The three most abundant orders detected were *Burkholderiales*, *Hydrogenophilales*, and *Rhizobiales*. The five most abundant genera detected were

Hydrogenophilus, Curvibacter, Tepidimonas, Anoxybacillus, and Pseudoxanthomonas (Fig. S2). Hydrogenophilus was the most abundant genus detected within nutrient addition incubation samples and was found in samples 274.55 NAN, 274.55  $\pm$  NP, 715.57  $\pm$  N, and 747.73 +NP. The six ASVs (ASVs 20 to 25) (Table S6) classified as Hydrogenophilus were identical at the nucleotide level to other Hydrogenophilus species commonly detected in geothermal environments (37-39). ASV14, classified as Curvibacter, was 99.73% identical to an uncultured bacterium isolated from a subsurface thermal spring in Franz-Josef springs (40). ASV54 was found to be 100% identical to Tepidimonas fonticaldi, isolated from hot spring systems (41-43). Hierarchical clustering of the community in incubation samples reveals no major grouping and no consistent trends with respect to any factor (Fig. S4). For every depth with 16S rRNA analysis of a core sample and nutrient addition incubation, ASV counts were higher in the core samples (Table S9).

Methane production in nutrient addition incubation experiments. The average methane production for all samples and treatments at 25 weeks, and between 25 to 60 weeks, was  $1.69 \times 10^{-2}$  nmol CH<sub>a</sub>·(g rocks·day)<sup>-1</sup> and 2.02 nmol CH<sub>a</sub>·(g rocks·day)<sup>-1</sup>, respectively. The means for these measurements were not statistically different for the two time points (P > 0.05). There are no killed controls for the nutrient incubation experiments, but the average methane production in samples between 25 and 60 weeks is higher than the average blank (artificial seawater [ASW] only) for methane production between 25 and 60 weeks of  $5.77 \times 10^{-4}$  nmol day<sup>-1</sup> (Fig. 5). There is a negative correlation between methane production at 25 weeks and carbonate vein frequencies, felsic vein frequencies, and total vein frequencies (correlation coefficients, -0.045, -0.23, and -0.19;  $R^2$  values, 0.0020, 0.054, and 0.038, respectively; Table S7). Between 25 and 60 weeks, there is a moderate positive correlation between average methane production and carbonate vein frequencies, a negative correlation for felsic vein frequencies, and a negligible correlation for total vein frequencies (correlation coefficients, 0.50, -0.26, and 0.12;  $R^2$  values, 0.25, 0.068, and 0.014). There is no significant trend of increased methane production with increased nutrient or organic carbon addition. For methane production at both 25 and 60 weeks, it was found that the effect of each treatment on methane production is not statistically different (ANOVA, *P* > 0.05) (Table S8).

# **DISCUSSION**

# Correlation between microbial abundance, diversity, and presence of veins.

The convective circulation of seawater in the subseafloor aguifer through fractures in the rocks creates a mechanism by which microbes can be dispersed (44, 45). The presence of felsic veins, carbonate veins, clay minerals, and open spaces (up to 7 mm in mean vein perpendicular thickness) within the gabbroic basement samples obtained from Hole U1473A provides evidence of low-temperature hydrothermal alteration and past and/or present fluid flow (19). Regardless of original formation temperatures, veins of all types with open spaces provide current potential conduits for fluids (46, 47). Carbonate veins form when seawater percolates through rocks, and felsic veins are formed during flow of magma. Access to fluids can make it possible for microbes that colonize surfaces and cracks to move and obtain nutrients. If access to fluids is subsequently cut off, microbes trapped within those features may persist for an undetermined period of time, provided basal energy requirements can be met. This has been shown for organic-poor, clay-rich, 101.5-million-year-old South Pacific Gyre sediments, where the high percentages of active cells in microaerobic incubations indicate that the resident microbial communities are metabolically active in situ (48).

Mean cell densities in cores recovered from Hole U1473A were  $6.18 \times 10^2$  cells cm<sup>-3</sup>. Similarly, abundances detected in shallow gabbroic basement samples at Atlantis Massif ranged from <10 to  $6.5 \times 10^2$  cells cm<sup>-3</sup>, and basaltic rock cell abundances from North Pond, on the west flank of the Mid-Atlantic Ridge, ranged from  $1.0 \times 10^3$  to  $6.1 \times 10^4$ cells cm<sup>-3</sup> (10, 16). Cell abundances at these disparate sites were in the same range and were also heterogeneous, indicating that low-biomass (≤10<sup>4</sup> cells cm<sup>-3</sup>), heterogeneously distributed populations may be the normal pattern for subseafloor igneous basement. Recently developed preservation and staining methods revealed that cell abundances may be as high as 10<sup>10</sup> cells cm<sup>-3</sup> locally at interfaces between clays and basalt (49) in basaltic

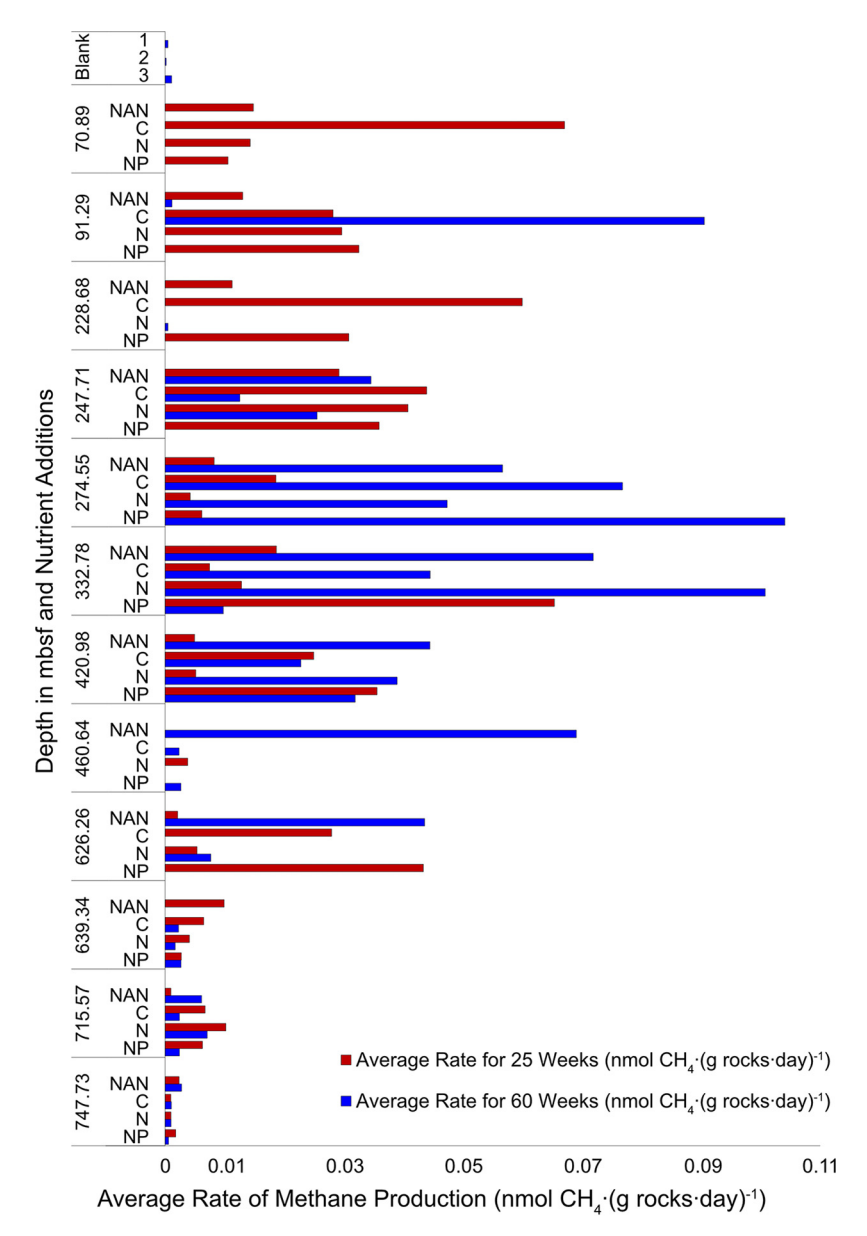


**FIG 5** Rate of methane production in nutrient addition incubation experiments. The rate at 25 weeks was derived from the value measured at 25 weeks minus the initial value (0) divided by the time elapsed in days. The rate at 60 weeks was derived from the difference between methane measured at 60 weeks and methane measured at 25 weeks divided by the time elapsed since the 25-week measurement. NAN, no added nutrients; C, carbon (lactate, acetate, and formate) addition; N, ammonium addition; NP, ammonium and phosphate addition.

basement >33.5 Ma, revealing extreme heterogeneity in cell densities depending on where and how sampling is conducted. This also suggests that local cell densities in igneous basement are significantly influenced by access to water and nutrients.

Carbonate vein frequency and cell counts were strongly correlated for depth ranges 268.16 to 332.78 and 432.84 to 522.73 mbsf, while felsic vein frequency showed a strong positive correlation with cell counts from 411.74 to 460.64 mbsf. However, the highest cell abundances in our study (10<sup>4</sup> cells cm<sup>-3</sup>) were observed at 247.71 mbsf, a depth not strongly correlated with vein frequencies. The scales at which cell counts and vein frequencies were recorded were vastly different and could explain why cell concentrations are not higher in samples with higher recorded vein frequencies. Samples obtained for microbiology during Expedition 360 were heterogeneous along the depth of Hole U1473A in terms of regions of alteration, mineral composition, and presence of veins and fractures.

When available,  $\sim$ 8- to 20-cm whole-round samples from within each 10-m core section were prioritized for microbiology studies that had the greatest evidence of fracturing and/or presence of veins and/or alteration. Vein frequencies, however, were not recorded at this scale; they were recorded for every 10 m of core sample. The amount of each rock sample used for cell counts was roughly 1 cm<sup>3</sup>, which is a significantly smaller scale than the 10-m core section used to quantify vein frequencies. Veins described for the 10-m section may therefore not reflect the densities or characteristics in the particular 1 cm<sup>3</sup> of rock from within that 10-m section that was used for cell counts or diversity analyses. Rock heterogeneity invariably creates regions within the rock more or less suitable for colonization by microorganisms, and therefore, we cannot rule out the possibility that our cell counts may miss locally higher regions of cell abundance in a sample, such as those recently detected by Suzuki and colleagues (49). In addition, drilling subseafloor basement inevitably results in the total loss of certain drilling depth intervals, often those with high concentrations of veins or high permeability, which may host high cell concentrations.

Sample heterogeneity explains not only the mismatch between cell counts and vein frequency but also the lack of a significant effect on different vein characteristics such as vein connectivity on the calculated average cell counts. For example, we would expect to see higher cell counts in network veins versus single veins. Ultimately, the patterns observed are not significantly shaped by any of the measured parameters and are most likely influenced by the downcore heterogeneity of the rock samples. At North Pond, cell abundances showed a strong positive correlation to porosity, suggesting that microbial abundance in subsurface basalts can be controlled by geophysical or geochemical changes (10). The heterogenous nature of the samples from Hole U1473A presents a challenge to identifying the effect of additional parameters on cell abundances.

The microbial community in recovered cores from Atlantis Bank was comprised of putative taxa that included many found in the marine water column, such as SAR11, SAR406, and Marinimicrobia (Fig. 3). It is possible that they were introduced into the lower oceanic crust by the circulation of seawater through the crust. Nitrosopumilales were abundant in almost all the core samples, and the Nitrosopumilales ASVs detected in Atlantis Bank samples were highly similar to uncultured archaeon clones isolated from a hydrothermal vent field along the SWIR. Likewise, the SAR11 ASVs were identical to an uncultured bacterium clone from the water column of the southwest Indian Ocean (33, 34). This indicates that the taxa could have been introduced from nearby environments via circulation of local seawater. One source of seawater to cored rocks recovered from Hole U1473A could be the fault zone of ~465 mbsf that was detected during drilling operations and drilled through but not cored (18). This fault may be a conduit of water flow into the massif from its side. The taxa present in the cored samples such as Nitrosopumilales and SAR406 point to potential metabolisms employed by the microbial community in the subsurface environment of Hole U1473A such as ammonia oxidation, sulfur reduction, and nitrate reduction (50-52). However, the limited and ephemeral carbon and energy resources ultimately determine the metabolic pathways for the microbial communities at this site (31).

Prokaryotic diversity showed a very strong positive correlation with vein frequencies (0.81 to 0.96) for the depth ranges of 119.72 to 182.44 and 600.51 to 682.32 mbsf (Table S4 in the supplemental material). However, when analyzing all the depth ranges together, the correlations are greatly reduced. Still, the ranges of positive correlations indicate an important link between vein frequency and diversity. Higher vein frequencies suggest a larger surface area present within the subsurface where microbes can travel, grow, and colonize. The strong positive correlations suggest that higher vein frequencies likely allow for different microbes to colonize due to larger spatial availability and potentially greater niche space, though the heterogeneity of the samples present a challenge in confirming this positive correlation throughout all depth ranges.

Effect of nutrient additions on the microbial community in incubation experiments. Hierarchical clustering of the microbial community in nutrient addition experiments did not reveal any consistent patterns (Fig. S4), resultant from the sparsity of the ASVs data set and highly abundant genera at a particular depth often being present in only

one of the treatments (Fig. S2). This inconsistency in the presence of certain genera is most likely due to the heterogeneity of the rocks, meaning that the presence of specific microbial populations is likely dictated by the spatial availability in the rocks, mineralogy, or other chemical and/or physical variation not detectable at the resolution of currently available methods or factors not assessed here. It could also be due to low microbial abundances in the samples and variable success in survival by lineages in the incubations. The low number of ASVs detected (57 ASVs after quality control) could also be attributed to extremely slow growth. Recent cultivation experiments describe the long incubation timelines required to grow certain isolates. One example of this cultivation from deep marine sediment is with the isolation of Candidatus Prometheoarchaeum syntrophicum (53). The cultivation and isolation efforts for this Archaea species extended over a decade. Another cultivation attempt that spanned over 2 years was with Candidatus Desulforudis that was originally isolated from a deep gold mine (54). These experiments suggest that the timeline of our nutrient addition incubation experiments may not be long enough to allow for the detection of prokaryotes from subsurface environments that require a significantly longer growth time.

The community structure in the collected cores and incubation samples differ entirely. While some orders overlap (Fig. 6), no ASVs were detected in both core samples and nutrient addition incubations. The primary difference between the core and incubation samples is that archaeal ASVs were not detected in the incubation samples. The most abundant orders in the core samples were Nitrosopumilales, SAR11, and SAR406, while the most abundant orders in the incubation samples were Burkholderiales, Hydrogenophilales, and Rhizobiales. Slow-growing Archaea are difficult to maintain in culture, and it is possible that Archaea were initially present but did not survive during our experiments. From the 12 depths for the nutrient addition experiments, ASV counts were available for 9 depths. In addition to a lack of overlap between the cored samples and incubations, ASV counts in all nutrient addition incubation samples were lower than ASV counts from the corresponding cored samples (Table S9).

ASVs classified as Hydrogenophilus were abundant in four of the nutrient addition incubations from three depths (Fig. 4). Hydrogenophilus are aerobic, moderately thermophilic, facultative chemolithoautotrophs that can grow autotrophically on hydrogen or sulfur compounds as the electron donor and carbon dioxide as the carbon source, or heterotrophically in organic media (39). Another ASV present in the incubation samples classified as Chroococcidiopsis is also a genus that is implicated in hydrogen oxidation in subsurface environments (55). In addition, Marinimicrobia, a taxon known for H oxidation (56), was detected in all the core samples, and mRNA from Chroococcidiopsis was also detected in the core samples, indicating they are active in this environment (31). Taken all together, H oxidation appears to be an important metabolic function in the Atlantis Bank subsurface.

We hypothesized that nutrient amendments would positively enhance community diversity in subseafloor samples from Atlantis Bank but did not find this to be the case. There is support for our findings from other recent work. In a multiyear mineral incubation study conducted using sterilized minerals incubated in subseafloor basaltic crust, nitrate was not found to be a limiting nutrient for biomass, though the addition of nitrate did cause a shift in the microbial community structure (57). This mirrors our lack of correlation with nutrient amendment treatment and indicates that the nutrients tested in these studies may not limit biomass in subseafloor basement. In a different study using terrestrial subsurface samples from Finnish crystalline bedrock, attempts to enrich acetoclastic methanogens resulted in no detected methanogens (58). The authors, however, did see a significant and near-complete shift in microbial community composition after 68 days of incubation and postulated that long-term enrichment incubations can drive a succession process where certain detritivore taxa flourish after the cell death of other taxa. Studies from the sedimentary deep biosphere also reveal heterogeneity in the response of the microbial community when introduced to various incubation experimental treatments (48, 59). Thirty-month-long stable isotope probing experiments from a coal bed 2 km below the seafloor found that the variation in metabolic activity in response to the different methyl compounds, presence/absence

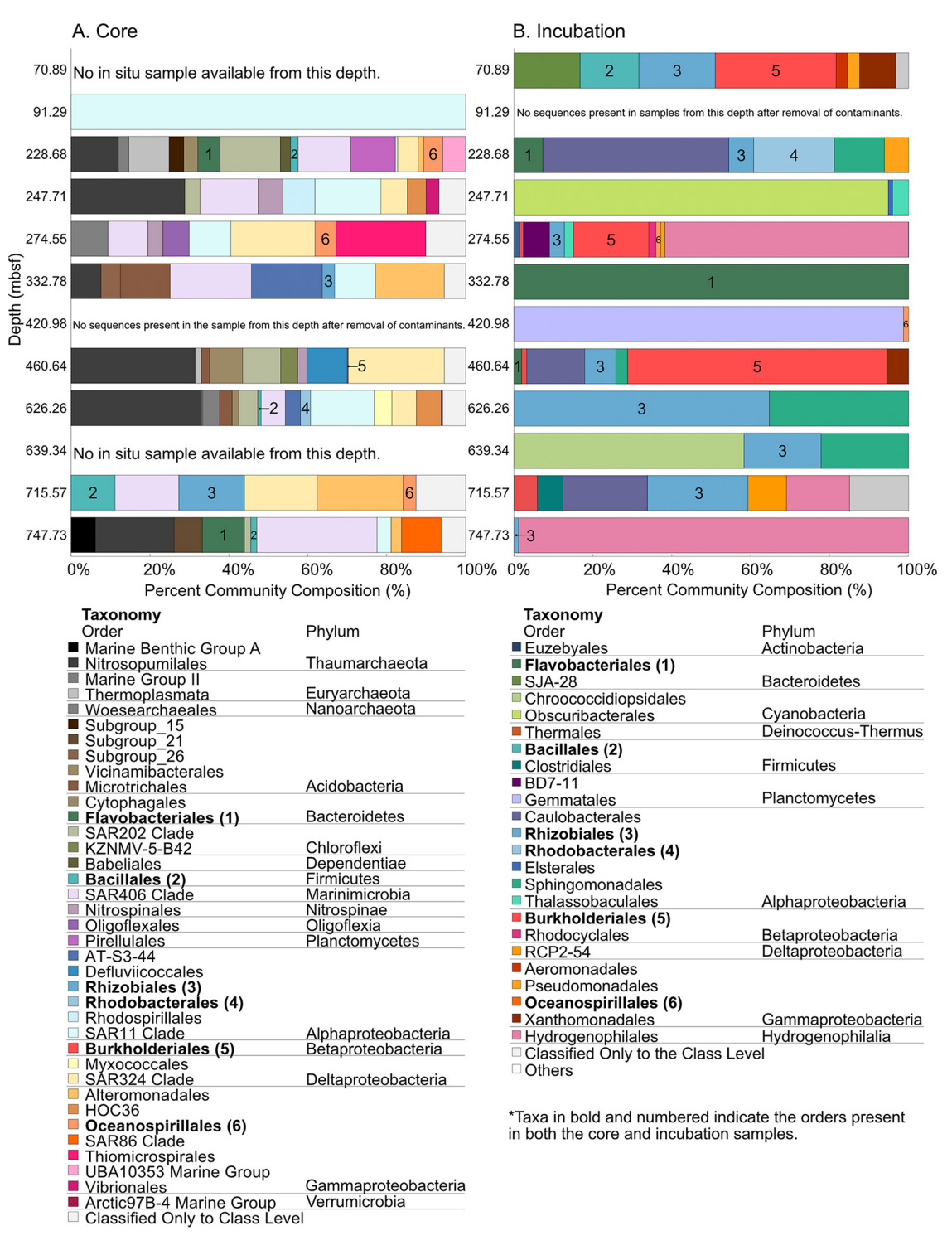


FIG 6 Microbial community composition on the order and phylum levels for core samples from the 12 depths that were included in the nutrient addition incubation experiments (A) and all combined samples from nutrient addition incubation experiments performed using material from each depth (B).

of hydrogen, and high temperature/pressure depicts a heterogenous microbial community (59). In a different study, microaerobic incubation experiments were set up with stable isotope-labeled substrates as tracers for microbial anabolic activities using sediments from the South Pacific Gyre. While the substrates generally supported biomass growth, the microbial metabolic response was heterogenous, and the rate of labeled isotope incorporation varied from one labeled substrate to another (48).

Effect of nutrient additions on methane production. Methane was detected in the headspace of incubations at levels above those measured in blank samples that contained ASW only. No killed controls are present in the nutrient addition incubation experiments, and thus, abiotic methane production was not able to be determined. Despite the detection of methane, no methanogens were detected. This is not unprecedented. For example, multiple lines of evidence pointed to the presence of methanogenic Archaea at IODP Site C0020, but only one archaeal 16S rRNA gene sequence related to a known methanogen was amplified, and archaeal 16S rRNA genes were not quantifiable by digital PCR (60). In addition, PCR may fail to amplify major archaeal lineages from poorly studied habitats due to sequence mismatches using domain-specific primers (61-63). That said, the primers used here were specifically designed to more efficiently amplify common Archaea in seawater (64), so it is possible that the low recovery in the nutrient addition experiments is real.

One-way ANOVA analysis revealed that the different nutrient additions did not enhance methane production within 0 to 25 weeks nor from 25 to 60 weeks. It was hypothesized that the addition of organic carbon sources, specifically lactate, acetate, and formate, would enhance methane production because these are common substrates that are used in acetoclastic methanogenesis. Though acetoclastic methanogenesis is responsible for biogenically produced methane in numerous environmental settings, only two genera from the order Methanosarcinales can utilize acetate to form methane (65-67). The lack of Methanosarcinales in these samples could explain why the carbon addition samples did not show increased methane production, although, as discussed above, it is possible that they were present but not detected. If there are methanogens present in the incubations, albeit undetected with 16S rRNA gene analysis, it is also possible that the majority are not from the order Methanosarcinales and instead employ hydrogenotrophic methanogenesis. In this case, methane production could be positively linked to higher olivine content in the rocks, as H<sub>2</sub> is a product of serpentinization from olivine reacting with water.

While abiotic production of methane via serpentinization is said to be extremely limited in temperatures below 200°C due to kinetic inhibitions, there could be other explanations for the presence of methane that is not biogenically produced, such as the presence of volatiles released from fluid inclusions exposed on rock surfaces as well as thermal breakdown products of potential contaminant organic compounds in the rocks (68, 69). Methane can possibly be occluded in widespread microfractures and porous serpentine- or chlorite-filled veins for chromitites and gabbros or peridotites in contact with chromitites (70). Additionally, methane produced from the reduction of inorganic carbon in secondary fluid inclusions within olivine possibly constitutes one of the largest reservoirs of methane on Earth and represents a significant source of abiotic methane in subsurface systems—concentrations of  $CH_4$  can range from 72 to 310 nmol  $CH_4$   $g^{-1}$  of gabbro in fluid inclusions hosted in olivine, plagioclase, and clinopyroxene (68). In Hole U1473A, olivine gabbro represents 76.5% of the U1473A core (19). While the area and volume of fluid inclusions are not known, if one assumes 76.5% of an idealized rock sample from U1473A to be olivine gabbro and uses the lower end of CH<sub>4</sub> concentrations in gabbro fluid inclusions of 72 nmol  $CH_4$   $g^{-1}$ , then there could be 55 nmol  $CH_4$   $g^{-1}$  of gabbro. It is unclear if this would be released on the time scale of our incubations, but this idealized calculation indicates that there is potentially enough CH<sub>4</sub> present in the rocks themselves to account for the highest measurement of methane in our incubation samples, 27 nmol CH<sub>4</sub> g<sup>-1</sup> (this value was obtained from sample 274.55 +NP and represents the total CH<sub>4</sub> measured between 25 and 60 weeks, without dividing by the days of incubation for an average rate measurement such as that shown in Fig. 5).

Correlation between methane production and vein frequency. Methane production showed a weak positive correlation to vein frequency, but only for the time range of 25 to 60 weeks (Table S7). This indicates that vein frequencies might not be the factor that enhances methane production, or if they do, their influence is more important over longer timescales. Higher vein density creates more interfaces for water-rock reactions.

Therefore, the correlation between vein frequency and methane produced could also be related to the availability to resident microbes of H<sub>2</sub> produced from serpentinization occurring in veins, or it could be related to exposure of fluid inclusions in our incubations, resulting in CH<sub>4</sub> release from the inclusions.

Conclusions. Subsurface rock samples are heterogeneous in nature, and this translated into heterogeneously distributed cell abundances and prokaryotic diversity that did not display strong statistical patterns. Microbial abundance and diversity along the depth of the core did show strong positive correlation to vein frequency at a few depth ranges, though this correlation is greatly reduced when viewed at a coarser level for all depths. The different nutrients added to the incubation experiments did not shape the microbial diversity or methane production in a predictable manner, and vein frequency only showed a weak positive correlation with methane production. In addition, the microbial community present in the cored rocks and incubation samples differed greatly, likely due to the transformation of the microbial community as it adapts to the change in nutrient type and availability over a long-term incubation. However, taken together, this study provides important insight into a very rarely studied biome via access to a long, continuous borehole. The results here provide data that can be used to predict patterns in community composition that may occur in lower oceanic crust sampled in other parts of the subseafloor with similar connectivity to fluid flows, as well as insight into what type of microorganisms could potentially survive in similar environments elsewhere in the solar system where silicate rocks and water are in contact.

#### **MATERIALS AND METHODS**

Sample collection. Onboard IODP Expedition 360, whole-round samples were selected from 10-m whole-round core sections for dedicated microbiology investigation within minutes of retrieval and immediately transferred into a sterile Whirlpak bag and transported to the microbiology laboratory for processing (19, 31). Once in the microbiology laboratory, the whole-round sample was rinsed four times in sterile water (changing the Whirlpak bag once after the second rinse) to reduce contamination from drilling fluid. The sample was then transferred to an ethanol-sterilized metal rock box placed within a positive-pressure clean area (19). The outside of each core was sprayed with 75% to 95% ethanol, wiped with Kimwipes, and then sprayed one final time with ethanol and left to air dry ( $\sim$ 5 min). During the drying time, photographs of each side of the whole-round sample were taken while it was sitting in the rock box. At all stages of the process, samples were handled as little as possible by a researcher wearing gloves, a lab coat, and a face mask. After cleaning the exterior of whole-round core samples, the rock was split with a sterile chisel, and core interiors were subsampled for postexpedition investigations (71). The exterior and interior samples of cores were analyzed using gas chromatography-mass spectrometry to determine if tracers (indication of contaminating drill fluids) were present; tracer concentrations suggested little to no contamination during sampling (31).

Cell separation and quantification. Paraformaldehyde (4 ml; 4% solution in 100 mM phosphatebuffered saline) was added to autoclaved 7-ml plastic tubes. Then, in the clean area, 1 ml of crushed rock material for each sample interior was added to a tube, bringing the total volume to 5 ml. Two replicate tubes were prepared for cell counts for each sample, and, where possible, vein material alone was aliquoted into one sample, and whole-rock powder was aliquoted into the other. Preserved samples were stored at 4°C for onshore analysis. We used 51 samples spanning from 10.73 to 781.45 mbsf for cell counts, and out of these 51 samples, 16 samples had replicate counts.

For cell counts, 1 ml of the fixed sample slurry was used in the quantification procedure. Cell counts were conducted using the same method previously reported for a small subset of these samples (31), based on a cell extraction and enumeration method developed for quantifying microbial abundance in subseafloor sediments (72). Briefly, the slurry was added to a detergent mix in a 15-ml centrifuge tube and shaken for 60 min. The centrifuge tube was then sonicated for 40 cycles using a Bioruptor sonicator (Diagenode, Denville, NJ) to release cells attached to the powdered rock. The solution was then laid on top of a density gradient with 30%, 50%, and 80% Nycodenz underlain by 67% sodium polytungstate. This gradient was next spun in a swing arm centrifuge at  $10,000 \times q$  for 60 min, after which the supernatant was removed to a 50-ml tube. The remaining rock debris was then transferred to a new tube and the entire procedure repeated, transferring the final step into the same 50-ml tube. The combined supernatants were then filtered onto 0.20-um-pore-size polycarbonate filters that were stained with a 1:40 dilution of the stock SYBR green I in Tris-EDTA (TE) buffer. Cells were enumerated on an epifluorescence microscope (Zeiss Axio Imager M2) by counting either 400 fields of view if fewer than a total of 40 cells were detected or at least 40 to 50 cells in fewer fields when possible. All cell counts were performed at Texas A&M University using a class ~10,000, overpressured cleanroom designed for work with low-biomass samples. A particle counter is deployed inside the room to monitor particles in the air that might cause contamination. This counter typically reads between 5,000 and 10,000 particles per square foot in open air. A Labconco Logic biosafety cabinet is located in the cleanroom, and samples were only opened in this cabinet, where particle counts are regularly zero. During sample handling, a static disruptor is kept turned on to reduce the likelihood of contaminating particles from the surrounding air, if present, landing on samples. The limit of quantification for cell counts from Expedition 360, defined as 3 times the standard deviation of all blank counts (3.5% NaCl used instead of sample slurry for the cell extraction and counting protocol), was  $8.50 \times 10^{1}$  cells cm<sup>-3</sup>.

Nutrient addition incubation experiments setup. Microcosm experiments were initiated during Expedition 360 in 38-ml serum vials with sterile anaerobic artificial seawater (ASW) as the basal media for all nutrient addition incubations (Table S10 in the supplemental material) (71). The following four conditions were tested: (i) no added nutrients (NAN), (ii)  $+750 \mu M$  ammonium chloride (NH<sub>4</sub>Cl) (+N), (iii)  $+750 \mu M$  NH<sub>4</sub>Cl  $+50~\mu$ M potassium phosphate, dibasic (K,HPO<sub>4</sub>) (+NP), and (iv)  $+200~\mu$ M (each) lactate, acetate, and formate (+C). Approximately 1 to 5 cm³ of crushed rock chips, depending on sample availability, were transferred in the clean space work area to 38-ml serum vials and submerged in anaerobic ASW to a level equivalent to 27 ml total volume (rocks plus media). After the appropriate additions were made to the vials, they were sealed with sterile butyl stoppers and gassed with a mixture of 90% N<sub>2</sub>, 5% H<sub>2</sub>, and 5% CO<sub>2</sub>. Using consistent headspace volume allowed for quantitative analysis of methane. Nutrient addition incubations were kept at 10°C for the duration of the experiment, close to in situ temperatures measured in Hole U1473A. Incubations were initially sampled for headspace CH<sub>4</sub> 25 weeks after the start of the experiments and then again at 60 weeks after the start of the experiments. After 20 months of incubation, the rocks from the vials were frozen for subsequent DNA extraction. DNA was extracted from the rocks 12 months after the rocks were frozen. No killed controls were present in the nutrient addition incubation experiment.

DNA extraction procedure for rock core samples. For the U1473A core samples, DNA extraction was performed as outlined in reference 31. DNA was extracted from 43 samples using 20 to 40 g of powdered rocks, depending on the quantity available. A DNeasy PowerMax soil kit (Qiagen) was used according to the manufacturer's protocol. Modifications included three freeze-thaw treatments before the addition of soil kit solution C1, and each treatment consisted of 1 min in liquid nitrogen followed by 5 min at 65°C. Isopropanol precipitation was then performed overnight at 4°C to concentrate the extracted DNA. Whole-genome amplification was performed before PCR amplification of marker genes. Genomic DNA was amplified by multiple-displacement amplification using the REPLI-g single-cell kit (Qiagen) as described. Multiple-displacement amplification bias was minimized by splitting each wholegenome amplification sample into triplicate 16-µl reactions after 1 h of amplification and then resuming amplification for the manufacturer-specified 7 h (8 h total). DNA was also recovered from samples of drilling mud and drilling fluid (surface water collected during the coring process) for negative controls, as well as two kit control samples in which no sample was added, to account for any contaminants originating from either the DNeasy PowerMax soil kit or the REPLI-g single-cell kit. Rock core samples were sequenced at University of Delaware DNA Sequencing & Genotyping Center.

DNA extraction procedure for nutrient addition incubation experiments. For nutrient addition experiments, roughly 0.5 cm<sup>3</sup> of rocks from each vial were used in a DNA extraction using the MP Biomedical FastDNA spin kit for soil, with a final elution volume of 50  $\mu$ l. For both sets of samples, the V4-V5 region of the 16S rRNA gene was amplified with the 515F and 926R PCR primer pair (64). For the incubation samples, Q5 high-fidelity DNA polymerase (New England Biolabs Inc.) was used for PCR with an initial denaturation of 30 s at 98°C followed by 35 cycles of 10 s at 98°C, 30 s at 50°C, and 30 s at 72°C followed by a final extension at 72°C for 2 min. Upon completion of extraction and amplification, samples were pooled in equimolar concentrations and sequenced using Illumina MiSeq sequencing at Georgia Genomics Facility.

16S rRNA analysis and quality control steps. The sequenced reads for both U1473A core and incubation samples were analyzed with the DADA2 (Divisive Amplicon Denoising Algorithm 2) pipeline with Silva v132 to produce ASVs (73, 74). Before performing statistical analyses, ASVs that were present in negative and kit controls were removed. These controls include drill fluid, drill fluid seawater, seawater and tracer, surface water, drill mud, blank MoBio kit, and PCR whole-genome analysis (WGA) controls. Genera that were commonly found in PCR contamination were also removed (75, 76), and ASVs that were identical to potential contaminants as a result of NCBI BLAST analysis were removed as well (Table S11). Using the blastn suite of NCBI BLAST, the ASV sequences were entered into a nucleotide query to search for highly similar sequences (MEGABLAST) in the nucleotide collection standard database. The top three to five sequences that produced significant alignments from separate accessions were analyzed. The isolation source of the matched sequences was the primary factor in this screening. ASVs with matches to more than one sequence or organisms isolated from medical settings or human or terrestrial animal origin were considered potential contaminants and were removed from further analysis. Statistical analyses performed with the 16S rRNA sequences were conducted using the vegan and phyloseq packages in R (77, 78). For the incubation samples, NMDS analysis produced a low stress value ( $9.0 \times 10^{-5}$ ). The data set for the incubation samples was therefore normalized using the variance stabilizing transformation function in DEseq2 (79), and hierarchical clustering was performed in R using

Methane measurements. CH<sub>4</sub> in the headspace of the vials was measured using a gas chromatograph with a flame ionization detector (GC-FID). The gas in the headspace of the vials was extracted and measured using GC-FID, similar to previous protocols (80, 81). Calibrations were performed for the measurements using methane tanks at 0 ppm, 1.0 ppm, and 6.41 ppm, and the sample loop was flushed for 1 min prior to each calibration measurement. The syringe used to inject the gas samples into the GC-FID loop was flushed three times with the 90% N<sub>2</sub>, 5% H<sub>2</sub>, and 5% CO<sub>2</sub> gas mixture prior to each sample extraction and injection. One-way analysis of variance (ANOVA) was used for analyzing the effect of the different treatments on methane production.

Data availability. Data are publicly available through the National Center for Biotechnology Information Sequence Read Archive (SRA) at BioProject PRJNA497074 and sample accession numbers SRR8136794 to SRR8136814 (data previously published in reference 31) and BioProject PRJNA708326 and accession numbers SRR13926086 to SRR13926170 and SRR13926172 to SRR13926174.

### **SUPPLEMENTAL MATERIAL**

Supplemental material is available online only. SUPPLEMENTAL FILE 1, PDF file, 1.7 MB. **SUPPLEMENTAL FILE 2**, XLSX file, 0.04 MB. SUPPLEMENTAL FILE 3, XLSX file, 5.8 MB.

# **ACKNOWLEDGMENTS**

We thank the captain, crew, and all who sailed on JOIDES Resolution for IODP Expedition 360, whose support was essential. We also thank Heath Goertzen, Mackenzie Maserang, and Jeramy Dedrick for lab assistance during methane measurements.

This study was funded by National Science Foundation grants OCE-1658031 to V.P.E. and OCE-1658118 to J.B.S., the U.S. Science Support Program, and a postexpedition award from Columbia University to J.B.S.

#### **REFERENCES**

- 1. Cowen JP, Giovannoni SJ, Kenig F, Johnson HP, Butterfield D, Rappé MS, Hutnak M, Lam P. 2003. Fluids from aging ocean crust that support microbial life. Science 299:120–123. https://doi.org/10.1126/science.1075653.
- 2. Jungbluth SP, Grote J, Lin H-T, Cowen JP, Rappé MS. 2013. Microbial diversity within basement fluids of the sediment-buried Juan de Fuca Ridge flank. ISME J 7:161-172. https://doi.org/10.1038/ismej.2012.73.
- 3. Lever MA, Rouxel O, Alt JC, Shimizu N, Ono S, Coggon RM, Shanks WC, Lapham L, Elvert M, Prieto-Mollar X, Hinrichs K-U, Inagaki F, Teske A. 2013. Evidence for microbial carbon and sulfur cycling in deeply buried ridge flank basalt. Science 339:1305-1308. https://doi.org/10.1126/science.1229240.
- 4. Smith A, Popa R, Fisk M, Nielsen M, Wheat CG, Jannasch HW, Fisher AT, Becker K, Sievert SM, Flores G. 2011. In situ enrichment of ocean crust microbes on igneous minerals and glasses using an osmotic flow-through device. Geochem Geophys Geosyst 12:Q06007. https://doi.org/10.1029/ 2010GC003424.
- 5. Nigro OD, Jungbluth SP, Lin H-T, Hsieh C-C, Miranda JA, Schvarcz CR, Rappé MS, Steward GF. 2017. Viruses in the oceanic basement. mBio 8: e02129-16. https://doi.org/10.1128/mBio.02129-16.
- 6. Smith AR, Fisk MR, Thurber AR, Flores GE, Mason OU, Popa R, Colwell FS. 2017. Deep crustal communities of the Juan de Fuca Ridge are governed by mineralogy. Geomicrobiol J 34:147–156. https://doi.org/10.1080/01490451 .2016.1155001.
- 7. Ramírez GA, Garber AI, Lecoeuvre A, D'Angelo T, Wheat CG, Orcutt BN. 2019. Ecology of subseafloor crustal biofilms. Front Microbiol 10:1983. https://doi.org/10.3389/fmicb.2019.01983.
- 8. Jørgensen SL, Zhao R. 2016. Microbial inventory of deeply buried oceanic crust from a young ridge flank. Front Microbiol 7:820. https://doi.org/10 3389/fmicb 2016 00820.
- 9. Meyer JL, Jaekel U, Tully BJ, Glazer BT, Wheat CG, Lin H-T, Hsieh C-C, Cowen JP, Hulme SM, Girguis PR, Huber JA. 2016. A distinct and active bacterial community in cold oxygenated fluids circulating beneath the western flank of the Mid-Atlantic ridge. Sci Rep 6:22541. https://doi.org/10.1038/srep22541.
- 10. Zhang X, Feng X, Wang F. 2016. Diversity and metabolic potentials of subsurface crustal microorganisms from the western flank of the Mid-Atlantic Ridge. Front Microbiol 7:363. https://doi.org/10.3389/fmicb.2016.00363.
- 11. Tully BJ, Wheat CG, Glazer BT, Huber JA. 2018. A dynamic microbial community with high functional redundancy inhabits the cold, oxic subseafloor aquifer. ISME J 12:1-16. https://doi.org/10.1038/ismej.2017.187.
- 12. Seyler LM, Trembath-Reichert E, Tully BJ, Huber JA. 2021. Time-series transcriptomics from cold, oxic subseafloor crustal fluids reveals a motile, mixotrophic microbial community. ISME J 15:1192-1206. https://doi.org/10 .1038/s41396-020-00843-4.
- 13. Kashefi K, Lovley DR. 2003. Extending the upper temperature limit for life. Science 301:934–934. https://doi.org/10.1126/science.1086823.
- 14. Takai K, Nakamura K, Toki T, Tsunogai U, Miyazaki M, Miyazaki J, Hirayama H, Nakagawa S, Nunoura T, Horikoshi K. 2008. Cell proliferation at 122°C and isotopically heavy CH4 production by a hyperthermophilic methanogen under high-pressure cultivation. Proc Natl Acad Sci U S A 105: 10949-10954. https://doi.org/10.1073/pnas.0712334105.
- 15. Mason OU, Nakagawa T, Rosner M, Van Nostrand JD, Zhou J, Maruyama A, Fisk MR, Giovannoni SJ. 2010. First investigation of the microbiology of the deepest layer of ocean crust. PLoS One 5:e15399. https://doi.org/10 .1371/journal.pone.0015399.

- 16. Früh-Green GL, Orcutt BN, Rouméjon S, Lilley MD, Morono Y, Cotterill C, Green S, Escartin J, John BE, McCaig AM, Cannat M, Ménez B, Schwarzenbach EM, Williams MJ, Morgan S, Lang SQ, Schrenk MO, Brazelton WJ, Akizawa N, Boschi C, Dunkel KG, Quéméneur M, Whattam SA, Mayhew L, Harris M, Bayrakci G, Behrmann JH, Herrero-Bervera E, Hesse K, Liu HQ, Ratnayake AS, Twing K, Weis D, Zhao R, Bilenker L. 2018. Magmatism, serpentinization and life: insights through drilling the Atlantis Massif (IODP Expedition 357). Lithos 323:137-155. https://doi.org/10.1016/j.lithos.2018.09.012.
- 17. Motamedi S, Orcutt BN, Früh-Green GL, Twing KI, Pendleton HL, Brazelton WJ. 2020. Microbial residents of the Atlantis Massif's shallow serpentinite subsurface. Appl Environ Microbiol 86:e00356-20. https://doi.org/10 .1128/AEM.00356-20.
- 18. Dick HJB, MacLeod CJ, Blum P, Abe N, Blackman DK, Bowles JA, Cheadle MJ, Cho K, Ciazela J, Deans JR, Edgcomb VP, Ferrando C, France L, Ghosh B, Ildefonse B, John B, Kendrick MA, Koepke J, Leong J. a M, Liu C, Ma Q, Morishita T, Morris A, Natland JH, Nozaka T, Pluemper O, Sanfilippo A, Sylvan JB, Tivey MA, Tribuzio R, Viegas G. 2019. Dynamic accretion beneath a slowspreading ridge segment: IODP Hole 1473A and the Atlantis Bank Oceanic Core Complex. J Geophys Res Solid Earth 124:12631–12659. https://doi.org/10 .1029/2018JB016858
- 19. Dick HJB, MacLeod CJ, Blum P, Expedition 360 Scientists. 2016. Proceedings of the International Ocean Discovery Program Volume 360 Expedition Reports. http://publications.iodp.org/proceedings/360/101/360\_101
- 20. Dick HJB, Lin J, Schouten H. 2003. An ultraslow-spreading class of ocean ridge. Nature 426:405-412. https://doi.org/10.1038/nature02128.
- 21. Snow J, Edmonds H. 2007. Ultraslow-spreading ridges: rapid paradigm changes. Oceanog 20:90-101. https://doi.org/10.5670/oceanog.2007.83.
- 22. Chen S, Shao Z. 2009. Isolation and diversity analysis of arsenite-resistant bacteria in communities enriched from deep-sea sediments of the Southwest Indian Ocean Ridge. Extremophiles 13:39–48. https://doi.org/10.1007/s00792 -008-0195-1.
- 23. Ding J, Zhang Y, Wang H, Jian H, Leng H, Xiao X. 2017. Microbial community structure of deep-sea hydrothermal vents on the ultraslow spreading Southwest Indian Ridge. Front Microbiol 8:1012. https://doi.org/10.3389/ fmicb.2017.01012.
- 24. Kröncke I, Tan TLok, Stein R. 1994. High benthic bacteria standing stock in deep Arctic basins. Polar Biol 14:423-428. https://doi.org/10.1007/BF00240263.
- 25. Li J. Peng X. Zhou H. Li J. Sun Z. 2013. Molecular evidence for microorganisms participating in Fe, Mn, and S biogeochemical cycling in two lowtemperature hydrothermal fields at the Southwest Indian Ridge. J Geophys Res Biogeosci 118:665-679. https://doi.org/10.1002/jgrg.20057.
- 26. Takai K, Gamo T, Tsunogai U, Nakayama N, Hirayama H, Nealson KH, Horikoshi K. 2004. Geochemical and microbiological evidence for a hydrogen-based, hyperthermophilic subsurface lithoautotrophic microbial ecosystem (HyperSLiME) beneath an active deep-sea hydrothermal field. Extremophiles 8:269-282. https://doi.org/10.1007/s00792-004-0386-3.
- 27. Lecoeuvre A, Ménez B, Cannat M, Chavagnac V, Gérard E. 2021. Microbial ecology of the newly discovered serpentinite-hosted Old City hydrothermal field (southwest Indian ridge). ISME J 15:818–832. https://doi.org/10 .1038/s41396-020-00816-7.
- 28. Kelley DS, Karson JA, Früh-Green GL, Yoerger DR, Shank TM, Butterfield DA, Hayes JM, Schrenk MO, Olson EJ, Proskurowski G, Jakuba M, Bradley

- A, Larson B, Ludwig K, Glickson D, Buckman K, Bradley AS, Brazelton WJ, Roe K, Elend MJ, Delacour A, Bernasconi SM, Lilley MD, Baross JA, Summons RE, Sylva SP. 2005. A serpentinite-hosted ecosystem: the lost city hydrothermal field. Science 307:1428-1434. https://doi.org/10.1126/science.1102556.
- 29. Martin W, Baross JA, Kelley DS, Russell MJ. 2008. Hydrothermal vents and the origin of life. Nat Rev Microbiol 6:805-814. https://doi.org/10.1038/ nrmicro1991.
- 30. Schrenk MO, Brazelton WJ, Lang SQ. 2013. Serpentinization, carbon, and deep life. Rev Mineral Geochem 75:575-606. https://doi.org/10.2138/rmg .2013.75.18.
- 31. Li J, Mara P, Schubotz F, Sylvan JB, Burgaud G, Klein F, Beaudoin D, Wee SY, Dick HJB, Lott S, Cox R, Meyer LAE, Quémener M, Blackman DK, Edgcomb VP. 2020. Recycling and metabolic flexibility dictate life in the lower oceanic crust. Nature 579:250-255. https://doi.org/10.1038/s41586-020-2075-5.
- 32. Quemener M, Mara P, Schubotz F, Beaudoin D, Li W, Pachiadaki M, Sehein TR, Sylvan JB, Li J, Barbier G, Edgcomb V, Burgaud G. 2020. Meta-omics highlights the diversity, activity and adaptations of fungi in deep oceanic crust. Environ Microbiol 22:3950-3967. https://doi.org/10.1111/1462-2920.15181.
- 33. Li J, Zhou H, Fang J, Wu Z, Peng X. 2016. Microbial distribution in a hydrothermal plume of the Southwest Indian Ridge. Geomicrobiol J 33: 401-415. https://doi.org/10.1080/01490451.2015.1048393.
- 34. Jiang X, Jiao N. 2016. Vertical distribution of bacterial communities in the Indian Ocean as revealed by analyses of 16S rRNA and nasA genes. Indian J Microbiol 56:309-317. https://doi.org/10.1007/s12088-016-0585-5.
- 35. Rogers AD, Tyler PA, Connelly DP, Copley JT, James R, Larter RD, Linse K, Mills RA, Garabato AN, Pancost RD, Pearce DA, Polunin NVC, German CR, Shank T, Boersch-Supan PH, Alker BJ, Aguilina A, Bennett SA, Clarke A, Dinley RJJ, Graham AGC, Green DRH, Hawkes JA, Hepburn L, Hilario A, Huvenne VAI, Marsh L, Ramirez-Llodra E, Reid WDK, Roterman CN, Sweeting CJ, Thatje S, Zwirglmaier K. 2012. The discovery of new deepsea hydrothermal vent communities in the southern ocean and implications for biogeography. PLoS Biol 10:e1001234. https://doi.org/10.1371/ journal.pbio.1001234.
- 36. Allers E, Wright JJ, Konwar KM, Howes CG, Beneze E, Hallam SJ, Sullivan MB. 2013. Diversity and population structure of marine group A bacteria in the northeast subarctic Pacific Ocean. ISME J 7:256-268. https://doi .org/10.1038/ismej.2012.108.
- 37. Hayashi NR, Ishida T, Yokota A, Kodama T, Igarashi Y. 1999. Hydrogenophilus thermoluteolus gen. nov., sp. nov., a thermophilic, facultatively chemolithoautotrophic, hydrogen-oxidizing bacterium. Int J Syst Bacteriol 49(Pt 2):783-786. https://doi.org/10.1099/00207713-49-2-783.
- 38. Vésteinsdóttir H, Reynisdóttir DB, Orlygsson J. 2011. Hydrogenophilus islandicus sp. nov., a thermophilic hydrogen-oxidizing bacterium isolated from an Icelandic hot spring. Int J Syst Evol Microbiol 61:290-294. https:// doi.org/10.1099/ijs.0.023572-0.
- 39. Arai H, Shomura Y, Higuchi Y, Ishii M. 2018. Complete genome sequence of a moderately thermophilic facultative chemolithoautotrophic hydrogenoxidizing bacterium, Hydrogenophilus thermoluteolus TH-1. Microbiol Resour Announc 7:e00857-18. https://doi.org/10.1128/MRA.00857-18.
- 40. Gerbl FW, Weidler GW, Wanek W, Erhardt A, Stan-Lotter H. 2014. Thaumarchaeal ammonium oxidation and evidence for a nitrogen cycle in a subsurface radioactive thermal spring in the. Austrian Central Alps. Front Microbiol 5:225. https://doi.org/10.3389/fmicb.2014.00225.
- 41. Jardine JL, Abia ALK, Mavumengwana V, Ubomba-Jaswa E. 2017. Phylogenetic analysis and antimicrobial profiles of cultured emerging opportunistic pathogens (phyla Actinobacteria and Proteobacteria) identified in hot springs. Int J Environ Res Public Health 14:1070. https://doi.org/10.3390/ijerph14091070.
- 42. Panda AK, Bisht SS, De Mandal S, Kumar NS. 2016. Bacterial and archeal community composition in hot springs from Indo-Burma region, North-east India. AMB Express 6:111. https://doi.org/10.1186/s13568-016-00284-y.
- 43. Tengku Abdul Hamid TH, Mohd Ghazali SA. 2015. New lipase producing β-proteobacteria strains Caldimonas sp. and Tepidimonas sp. isolated from a Malaysian hot springs. JSM 44:701–706. https://doi.org/10.17576/ jsm-2015-4405-09.
- 44. Orcutt BN, Wheat CG, Rouxel O, Hulme S, Edwards KJ, Bach W. 2013. Oxygen consumption rates in subseafloor basaltic crust derived from a reaction transport model. Nat Commun 4:2539. https://doi.org/10.1038/ncomms3539.
- 45. Whitman WB, Coleman DC, Wiebe WJ. 1998. Prokaryotes: the unseen majority. Proc Natl Acad Sci U S A 95:6578-6583. https://doi.org/10.1073/ pnas.95.12.6578.
- 46. Fisher AT, Becker K. 2000. Channelized fluid flow in oceanic crust reconciles heat-flow and permeability data. Nature 403:71-74. https://doi.org/ 10.1038/47463.

- 47. Fisher AT, Davis EE, Hutnak M, Spiess V, Zühlsdorff L, Cherkaoui A, Christiansen L, Edwards K, Macdonald R, Villinger H, Mottl MJ, Wheat CG, Becker K. 2003. Hydrothermal recharge and discharge across 50 km guided by seamounts on a voung ridge flank. Nature 421:618-621. https://doi.org/10.1038/nature01352.
- 48. Morono Y, Ito M, Hoshino T, Terada T, Hori T, Ikehara M, D'Hondt S, Inagaki F. 2020. Aerobic microbial life persists in oxic marine sediment as old as 101.5 million years. Nat Commun 11:3626. https://doi.org/10.1038/ s41467-020-17330-1.
- 49. Suzuki Y, Yamashita S, Kouduka M, Ao Y, Mukai H, Mitsunobu S, Kagi H, D'Hondt S, Inagaki F, Morono Y, Hoshino T, Tomioka N, Ito M. 2020. Deep microbial proliferation at the basalt interface in 33.5–104 million-year-old oceanic crust. Commun Biol 3:136. https://doi.org/10.1038/s42003-020-0860-1.
- 50. Könneke M, Bernhard AE, de la Torre JR, Walker CB, Waterbury JB, Stahl DA. 2005. Isolation of an autotrophic ammonia-oxidizing marine archaeon. Nature 437:543-546. https://doi.org/10.1038/nature03911.
- 51. Oin W. Heal KR, Ramdasi R, Kobelt JN, Martens-Habbena W, Bertagnolli AD, Amin SA, Walker CB, Urakawa H, Könneke M, Devol AH, Moffett JW, Armbrust EV, Jensen GJ, Ingalls AE, Stahl DA. 2017. Nitrosopumilus maritimus gen. nov., sp. nov., Nitrosopumilus cobalaminigenes sp. nov., Nitrosopumilus oxyclinae sp. nov., and Nitrosopumilus ureiphilus sp. nov., four marine ammonia-oxidizing archaea of the phylum Thaumarchaeota. Int J Syst Evol Microbiol 67:5067-5079. https://doi.org/10.1099/ijsem.0.002416.
- 52. Thrash JC, Seitz KW, Baker BJ, Temperton B, Gillies LE, Rabalais NN, Henrissat B, Mason OU. 2017. Metabolic roles of uncultivated bacterioplankton lineages in the Northern Gulf of Mexico "Dead Zone". mBio 8: e01017-17. https://doi.org/10.1128/mBio.01017-17.
- 53. Imachi H, Nobu MK, Nakahara N, Morono Y, Ogawara M, Takaki Y, Takano Y, Uematsu K, Ikuta T, Ito M, Matsui Y, Miyazaki M, Murata K, Saito Y, Sakai S, Song C, Tasumi E, Yamanaka Y, Yamaguchi T, Kamagata Y, Tamaki H, Takai K. 2020. Isolation of an archaeon at the prokaryote-eukaryote interface. Nature 577:519-525. https://doi.org/10.1038/s41586-019-1916-6.
- 54. Karnachuk OV, Frank YA, Lukina AP, Kadnikov VV, Beletsky AV, Mardanov AV, Ravin NV. 2019. Domestication of previously uncultivated Candidatus Desulforudis audaxviator from a deep aquifer in Siberia sheds light on its physiology and evolution. ISME J 13:1947-1959. https://doi.org/10.1038/ s41396-019-0402-3.
- 55. Puente-Sánchez F, Arce-Rodríguez A, Oggerin M, García-Villadangos M, Moreno-Paz M, Blanco Y, Rodríguez N, Bird L, Lincoln SA, Tornos F, Prieto-Ballesteros O, Freeman KH, Pieper DH, Timmis KN, Amils R, Parro V. 2018. Viable cyanobacteria in the deep continental subsurface. Proc Natl Acad Sci U S A 115:10702-10707. https://doi.org/10.1073/pnas.1808176115.
- 56. Hawley AK, Nobu MK, Wright JJ, Durno WE, Morgan-Lang C, Sage B, Schwientek P, Swan BK, Rinke C, Torres-Beltrán M, Mewis K, Liu W-T, Stepanauskas R, Woyke T, Hallam SJ. 2017. Diverse Marinimicrobia bacteria may mediate coupled biogeochemical cycles along eco-thermodynamic gradients. Nat Commun 8:1507. https://doi.org/10.1038/s41467-017-01376-9.
- 57. Orcutt BN, D'Angelo T, Wheat CG, Trembath-Reichert E. 2021. Microbemineral biogeography from multi-year incubations in oceanic crust at North Pond, Mid-Atlantic Ridge. Environ Microbiol 23:3923–3936. https:// doi.org/10.1111/1462-2920.15366.
- 58. Purkamo L, Bomberg M, Nyyssönen M, Ahonen L, Kukkonen I, Itävaara M. 2017. Response of deep subsurface microbial community to different carbon sources and electron acceptors during  $\sim\!2$  months incubation in microcosms. Front Microbiol 8:232. https://doi.org/10.3389/fmicb.2017.00232.
- 59. Trembath-Reichert E, Morono Y, Ijiri A, Hoshino T, Dawson KS, Inagaki F, Orphan VJ. 2017. Methyl-compound use and slow growth characterize microbial life in 2-km-deep subseafloor coal and shale beds. Proc Natl Acad Sci USA 114:E9206-E9215. https://doi.org/10.1073/pnas.1707525114.
- 60. Inagaki F, Hinrichs K-U, Kubo Y, Bowles MW, Heuer VB, Hong W-L, Hoshino T, Ijiri A, Imachi H, Ito M, Kaneko M, Lever MA, Lin Y-S, Methé BA, Morita S, Morono Y, Tanikawa W, Bihan M, Bowden SA, Elvert M, Glombitza C, Gross D, Harrington GJ, Hori T, Li K, Limmer D, Liu C-H, Murayama M, Ohkouchi N, Ono S, Park Y-S, Phillips SC, Prieto-Mollar X, Purkey M, Riedinger N, Sanada Y, Sauvage J, Snyder G, Susilawati R, Takano Y, Tasumi E, Terada T, Tomaru H, Trembath-Reichert E, Wang DT, Yamada Y. 2015. Exploring deep microbial life in coal-bearing sediment down to  $\sim$ 2.5 km below the ocean floor. Science 349:420-424. https://doi.org/10.1126/science.aaa6882.
- 61. Hoshino T, Inagaki F. 2019. Abundance and distribution of Archaea in the subseafloor sedimentary biosphere. ISME J 13:227-231. https://doi.org/ 10.1038/s41396-018-0253-3.
- 62. Lipp JS, Morono Y, Inagaki F, Hinrichs K-U. 2008. Significant contribution of Archaea to extant biomass in marine subsurface sediments. Nature 454:991-994. https://doi.org/10.1038/nature07174.

- 63. Teske A, Sørensen KB. 2008. Uncultured archaea in deep marine subsurface sediments: have we caught them all? ISME J 2:3-18. https://doi.org/ 10.1038/ismej.2007.90.
- 64. Parada AE, Needham DM, Fuhrman JA. 2016. Every base matters: assessing small subunit rRNA primers for marine microbiomes with mock communities, time series and global field samples. Environ Microbiol 18: 1403-1414. https://doi.org/10.1111/1462-2920.13023.
- 65. Ferry JG. 1992. Methane from acetate. J Bacteriol 174:5489-5495. https:// doi.org/10.1128/jb.174.17.5489-5495.1992.
- 66. Fournier GP, Gogarten JP. 2008. Evolution of acetoclastic methanogenesis in Methanosarcina via horizontal gene transfer from cellulolytic Clostridia. J Bacteriol 190:1124-1127. https://doi.org/10.1128/JB.01382-07.
- 67. Stams AJM, Teusink B, Souza DZ. 2019. Ecophysiology of acetoclastic methanogens, p 1-14. In Stams A, Sousa D (ed), Biogenesis of hydrocarbons. Handbook of hydrocarbon and lipid microbiology. Springer, Cham-
- 68. Klein F, Grozeva NG, Seewald JS. 2019. Abiotic methane synthesis and serpentinization in olivine-hosted fluid inclusions. Proc Natl Acad Sci U S A 116:17666-17672. https://doi.org/10.1073/pnas.1907871116.
- 69. McCollom TM. 2016. Abiotic methane formation during experimental serpentinization of olivine. Proc Natl Acad Sci U S A 113:13965-13970. https://doi.org/10.1073/pnas.1611843113.
- 70. Etiope G, Ifandi E, Nazzari M, Procesi M, Tsikouras B, Ventura G, Steele A, Tardini R, Szatmari P. 2018. Widespread abiotic methane in chromitites. Sci Rep 8:8728. https://doi.org/10.1038/s41598-018-27082-0.
- 71. MacLeod CJ, Dick HJB, Blum P, Abe N, Blackman DK, Bowles JA, Cheadle MJ, Cho K, Ciążela J, Deans JR, Edgcomb VP, Ferrando C, France L, Ghosh B, Ildefonse BM, Kendrick MA, Koepke JH, Leong JAM, Liu C, Ma Q, Morishita T, Morris A, Natland JH, Nozaka T, Pluemper O, Sanfilippo A, Sylvan JB, Tivey MA, Tribuzio R, Viegas LGF. 2017. Expedition 360 methods. In Proceedings of the International Ocean Discovery Program, vol 360. https://doi.org/10.14379/iodp.proc.360.102.2017.
- 72. Morono Y, Terada T, Kallmeyer J, Inagaki F. 2013. An improved cell separation technique for marine subsurface sediments: applications for high-

- throughput analysis using flow cytometry and cell sorting. Environ Microbiol 15:2841-2849. https://doi.org/10.1111/1462-2920.12153.
- 73. Callahan BJ, McMurdie PJ, Rosen MJ, Han AW, Johnson AJA, Holmes SP. 2016. DADA2: high-resolution sample inference from Illumina amplicon data. Nat Methods 13:581-583. https://doi.org/10.1038/nmeth.3869.
- 74. Rosen MJ, Callahan BJ, Fisher DS, Holmes SP. 2012. Denoising PCR-amplified metagenome data. BMC Bioinformatics 13:283. https://doi.org/10.1186/1471
- 75. Salter SJ, Cox MJ, Turek EM, Calus ST, Cookson WO, Moffatt MF, Turner P, Parkhill J, Loman NJ, Walker AW. 2014. Reagent and laboratory contamination can critically impact sequence-based microbiome analyses. BMC Biol 12:87. https://doi.org/10.1186/s12915-014-0087-z.
- 76. Sheik CS, Reese BK, Twing KI, Sylvan JB, Grim SL, Schrenk MO, Sogin ML, Colwell FS. 2018. Identification and removal of contaminant sequences from ribosomal gene databases: lessons from the census of deep life. Front Microbiol 9:840. https://doi.org/10.3389/fmicb.2018.00840.
- 77. McMurdie PJ, Holmes S. 2013. phyloseq: an R package for reproducible interactive analysis and graphics of microbiome census data. PLoS One 8: e61217. https://doi.org/10.1371/journal.pone.0061217.
- 78. Oksanen J, Blanchet FG, Friendly M, Kindt R, Legendre P, McGlinn D, Minchin PR, O'Hara RB, Simpson GL, Solymos P, Stevens MH, Szoecs E, Wagner H. 2019. vegan: community ecology package version 2.5-5 from CRAN. https://CRAN.R -project.org/package=vegan.
- 79. Love MI, Huber W, Anders S. 2014. Moderated estimation of fold change and dispersion for RNA-seg data with DESeg2. Genome Biol 15:550. https://doi.org/10.1186/s13059-014-0550-8.
- 80. Johnson KM, Hughes JE, Donaghay PL, Sieburth JM. 1990. Bottle-calibration static head space method for the determination of methane dissolved in seawater. Anal Chem 62:2408-2412. https://doi.org/10.1021/ac00220a030
- 81. Valentine DL, Kessler JD, Redmond MC, Mendes SD, Heintz MB, Farwell C, Hu L, Kinnaman FS, Yvon-Lewis S, Du M, Chan EW, Garcia Tigreros F, Villanueva CJ. 2010. Propane respiration jump-starts microbial response to a deep oil spill. Science 330:208-211. https://doi.org/10.1126/science.1196830.